

Reduced Pulsatile Trabecular Meshwork Motion in Eyes With Primary Open Angle Glaucoma Using Phase-Sensitive Optical Coherence Tomography

Kai Gao,^{1,3} Shaozhen Song,¹ Murray A. Johnstone,² Qinqin Zhang,¹ Jingjiang Xu,¹ Xiulan Zhang,³ Ruikang K. Wang,^{1,2} and Joanne C. Wen^{2,4}

¹Department of Bioengineering, University of Washington, Seattle, Washington, United States

²Department of Ophthalmology, University of Washington, Seattle, Washington, United States

³State Key Laboratory of Ophthalmology, Zhongshan Ophthalmic Center, Sun Yat-Sen University, Guangzhou, China

⁴Duke Eye Center, Durham, North Carolina, United States

Correspondence: Joanne C. Wen, Department of Ophthalmology, Duke Eye Center, 2351 Erwin Road, Durham, NC 27705, USA; joanne.wen@duke.edu.

Ruikang K. Wang, Department of Bioengineering, University of Washington, William H. Foege Building, 3720 15th Ave NE, Seattle, WA 98195, USA; wangrk@uw.edu.

Received: February 4, 2020

Accepted: November 24, 2020

Published: December 16, 2020

Citation: Gao K, Song S, Johnstone MA, et al. Reduced pulsatile trabecular meshwork motion in eyes with primary open angle glaucoma using phase-sensitive optical coherence tomography. *Invest Ophthalmol Vis Sci.* 2020;61(14):21. <https://doi.org/10.1167/iovs.61.14.21>

PURPOSE. The purpose of this study was to investigate the difference in pulsatile trabecular meshwork (TM) motion between normal and eyes with POAG using phase-sensitive optical coherence tomography (PhS-OCT).

METHODS. In this cross-sectional study, eight healthy subjects (16 eyes) and nine patients with POAG (18 eyes) were enrolled. A laboratory-based prototype PhS-OCT system was used to measure pulsatile TM motion. PhS-OCT images were analyzed to obtain parameters of pulsatile TM motion (i.e. maximum velocity [MV] and cumulative displacement [CDisp]). Outflow facility and ocular pulse amplitude were measured using pneumotonomography. Detection sensitivity was compared among various parameters by calculating the area under the receiver operating characteristic curves (AUCs).

RESULTS. A pulsatile TM motion waveform synchronous with digital pulse was observed using PhS-OCT in both healthy and POAG eyes. The mean MV in eyes with glaucoma was significantly lower than healthy eyes ($P < 0.001$). The mean CDisp in POAG eyes was also significantly lower than healthy eyes ($P < 0.001$). CDisp showed a significant correlation ($r = 0.46$; $P = 0.0088$) with ocular pulse amplitude in the study. Compared with the outflow facility, both the MV and CDisp were found to have a better discrimination of glaucoma ($P < 0.001$ and $P = 0.0074$, respectively).

CONCLUSIONS. Pulsatile TM motion was reduced in patients with POAG compared to healthy subjects. The underlying mechanism may be due to the altered tissue stiffness or other biomechanical properties of the TM in POAG eyes. Our evidence suggests that the measurement of pulsatile TM motion with PhS-OCT may help in characterizing outflow pathway abnormalities.

Keywords: trabecular meshwork, primary open angle glaucoma, phase-sensitive optical coherence tomography, pulsatile motion

Glaucoma is the leading cause of irreversible blindness worldwide, which is characterized by progressive loss of retinal ganglion cells that results in corresponding visual field (VF) defects.¹ POAG is the most prevalent form of glaucoma and elevated IOP is perhaps the most significant and modifiable risk factor.²⁻⁴ However, the cause of IOP elevation in POAG is less understood. IOP homeostasis depends on the normal function of the aqueous humor (AH) outflow system, consisting of the conventional and uveoscleral outflow pathways. Aqueous outflow facility, a measure of the ease of AH outflow through the outflow system, is often impaired in POAG, resulting in an abnormal IOP.⁵ Prior studies suggest that the majority of AH outflow resistance resides in the juxtacanalicular tissue (JCT) of trabecular meshwork (TM) and the inner wall of Schlemm's canal (SC).^{6,7} Furthermore, abnormalities of the TM in patients with POAG have been identified, including alterations in

the extracellular matrix (ECM) composition and the clearance ability of TM cells. These findings suggest that TM dysfunction plays a critical role in the pathogenesis of POAG.^{8,9}

The TM exhibits pulsatile motion resulting from the ocular pulse created by the cardiac cycle. TM stiffness is one of the factors that affects the pulsatile motion of the TM. This study's findings are consistent with TM dysfunction in patients with glaucoma, which may contribute to IOP dysregulation.^{8,10,11}

Phase-sensitive optical coherence tomography (PhS-OCT) has previously been used to quantify the pulsatile movement of the TM in vivo with high repeatability and reliability in healthy volunteers.¹² However, the pulsatile movement of the TM in POAG has yet to be evaluated. In this study, we ask: (1) is there a difference in pulsatile TM motion between healthy patients and patients with POAG? (2) Would

pulsatile TM motion be effective in predicting the presence of glaucoma?

To address these questions, we conducted this cross-sectional study to investigate the difference in pulsatile TM motion between healthy patients and patients with POAG.

METHODS

Subjects

This cross-sectional study was conducted at the University of Washington Medicine Eye Institute between September 2018 and June 2019. This study was approved by the Ethical Review Committee of University of Washington (Seattle, WA, USA). This study adhered to the tenets of the Declaration of Helsinki and was conducted in compliance with the Health Insurance Portability and Accountability Act (HIPAA). Written informed consent was obtained from all subjects.

All subjects received comprehensive ocular examinations that included a review of their medical history, best-corrected visual acuity, a slit-lamp examination, and a stereoscopic optic disc examination with a 90-diopter lens. Blood pressure (BP) was measured using an automatic BP device (Welch Allyn Spot Vital Signs, version 2; Welch Allyn Inc., Skaneateles Falls, NY, USA). We defined the mean arterial pressure (MAP) as diastolic BP plus one third times (systolic BP minus diastolic BP). IOP was measured using a portable rebound tonometer (iCare, ic100; iCare, Helsinki, Finland). Measurements of aqueous outflow facility and ocular pulse amplitude were obtained noninvasively by 2-minute tonography using a pneumotonometer per standard methods (Model 30; Reichert, Depew, NY, USA). The axial length (AL) and anterior chamber depth (ACD) were measured using partial coherence interferometry biometer (IOL Master, version 5.4; Carl Zeiss Meditec, La Jolla, CA, USA). POAG was defined as the presence of a normal open angle on gonioscopy, an untreated IOP of > 21 mm Hg, and glaucomatous optic nerve damage with a corresponding typical VF defect as confirmed by at least two reproducible VF tests.¹³ All patients with POAG received standard automated perimetry examination on a Humphrey Field Analyzer (Carl Zeiss Meditec, Dublin, CA, USA), and only reliable tests were accepted ($\leq 20\%$ fixation losses and false-positive and false-negative rates). Subjects were excluded if they: (1) had previous intraocular surgeries other than uncomplicated cataract surgery at least 6 months prior (e.g. laser trabeculoplasty or glaucoma surgery, etc.); (2) had other ocular diseases (e.g. uveitis, conjunctivitis, and fundus diseases); (3) had known cardiac arrhythmias; or (4) had myopia worse than a spherical equivalent of -4 diopters.

PhS-OCT Examination

An experienced investigator (K.G.) performed the PhS-OCT examinations in the same dimly lit room of stable illumination in the morning at approximately 10 AM. All participants were in a sitting position during PhS-OCT examinations. The laboratory PhS-OCT system prototype was comprised of three parts: a spectral domain OCT (SD-OCT) system, a digital pulsimeter, and an external controlling unit. The control unit was used to synchronize OCT data acquisition and cardiac signal recording, as described in our previous study.¹³ Briefly, the SD-OCT system used a superluminescent diode with a wavelength of 1310 nm as the light source with a spectral bandwidth of 100 nm, giving an axial reso-

lution of approximately 5.5 μm in tissue. The lateral resolution of approximately 16 μm was determined by the objective lens (50 mm focal length) used to focus the sample beam into the sample. A repeated B-scan pattern covering 3.5 mm was performed and that was centered on the temporal limbus. For each imaging session, 2000 OCT B-scans (400 B-scan/s) were captured, lasting for a duration of 5 seconds, which approximately covers 5 cardiac cycles. Because the TM movement is the target of the measurement in this investigation, the system sensitivity is a more important metric of concern. The metric is a measure of the smallest displacement that can be measured under the intrinsic system noise floor. The system noise floor was measured at approximately 15 mrad using an ex vivo cornea tissue to simulate in vivo anterior segment tissue. The measurement translates to a minimal displacement of approximately 1.2 nm that the SD-OCT system can measure (assuming that the average refractive index of the tissue is 1.35). Correspondingly, given the system imaging speed of 400 fps (i.e. $\Delta t = 2.5$ ms), the minimum resolvable velocity for the current phase sensitive SD OCT system is approximately 0.48 $\mu\text{m/s}$. For detailed information on how to characterize the OCT system for dynamic displacement measurement, please refer to the paper by Wang et al.¹⁴ Another pertinent concern is the issue of inevitable movement of the patient during imaging, which must be removed during the data processing. In dealing with this, we used a proprietary technique in which a phase compensation strategy is used to remove the bulk tissue movement induced by involuntary patient motion in the measurements. If readers are interested, please refer to the papers by An et al. for more details of this strategy.^{15,16}

During imaging, consistent positioning was achieved as follows. Patients' faces were oriented in a straight-ahead position. Patients then looked at an external fixation target without moving their head, placing the eye in an optimal position for the PhS-OCT to acquire images of the temporal limbus. An identical protocol was used for each participant. Three repeated scans were captured of each eye. A digital pulsimeter (TN1012/ST; AD Instruments Pty Ltd., Colorado Springs, CO, USA) was placed on the index finger of the participants, which was then used to record the signal from the cardiac pulse using LabChart Pro (version 8.1.11; AD Instruments Pty Ltd., Sydney, Australia). The data acquisition from the pulsimeter and PhS-OCT was synchronized by using a trigger signal provided by an external controlling unit (ML866, PowerLab 4/30; AD Instruments Pty Ltd., New South Wales, Australia).

Data Processing and Measurements of Pulsatile TM Motion

Each dataset contained 2000 cross-sectional OCT images of the scanned area. Minimization of bulk tissue motion artifacts and automatic alignment of adjacent B-scans were achieved using a proprietary algorithm.^{10,12} The velocity waveform of each pixel in the OCT image was generated as described in our previous study.¹² In brief: (1) the phase shift of each pixel in the OCT signal was calculated between adjacent B-scans, and then the instantaneous velocity was obtained by calculating the displacement between two B-scan images; (2) the velocity waveform during the scan period (5 seconds) was acquired on every pixel in the PhS-OCT image; (3) motion waveforms of every location were

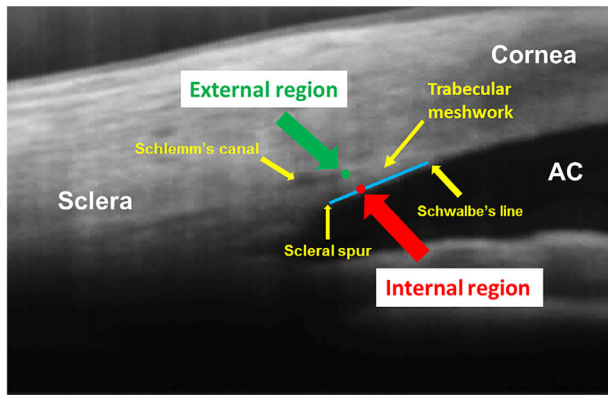


FIGURE 1. Regions and features targeted to measure in the optical coherence tomography (OCT) image containing outflow facility. A line was drawn between the sclera spur and Schwalbe's line. The position of the posterior one third of this line was defined as the internal region of the trabecular meshwork (TM) (red circle), and the adjacent green circle next to the Schlemm's canal indicated the external region of the TM. AC, anterior chamber.

generated in whole OCT image followed by use of a mask derived from the cardiac pulse and harmonic frequency filtered the motion waveforms in the frequency domain. The maximum velocity (MV) was defined as the maximum value on the velocity waveform, and cumulative displacement (CDisp) was defined as the integration of the velocity waveform within a cardiac cycle.

The PhS-OCT images were analyzed to determine both MV and CDisp of the pulsatile TM motion as follows¹² (Fig. 1): (1) a line was drawn between the scleral spur and Schwalbe's line on the interior inner surface of the cornea; (2) the internal inner region of the TM was chosen at one-third of the distance anterior to scleral spur along the line described in (1), then the value of internal MV (IMV) and internal CDisp (ICDisp) was calculated; (3) the external region of the TM was identified at the area next to Schlemm's canal opposite the internal location, then the value of the external MV (EMV) and external CDisp (ECDisp) were calculated; And (4) the values for MV and CDisp were calculated as the average of three acquired consecutive PhS-OCT images. The mean value for MV and CDisp of each eye was calculated as the average of the internal and external region of the TM, which were defined as MV_{mean} and $CDisp_{\text{mean}}$. All measurements were performed by an experienced investigator (K.G.), who was masked to the subject's clinical data.

Image analysis to measure the MV and CDisp of the TM was performed in two separate sessions over an interval of 2 weeks to assess the reproducibility of the pulsatile TM motion parameter measurements.

Statistical Analysis

Descriptive statistics were calculated as the means and standard deviations (mean \pm SDs). The significance of differences in parameters of pulsatile TM motion between normal and patients with POAG were determined using either an unpaired *t*-test or a Mann-Whitney *U* test based on the analysis of normality (Shapiro-Wilk test). The intraclass correlation coefficient (ICC) was used to demonstrate the repeatability and reproducibility of the pulsatile TM motion measurements in PhS-OCT images. Correlation

analysis among pulsatile TM motion parameters (i.e. IMV, EMV, and MV_{mean} , ICDisp, ECDisp, and $CDisp_{\text{mean}}$) and other ocular parameters (i.e. outflow facility and ocular pulse amplitude) was determined using Pearson correlation test. Receiver operating characteristic (ROC) curves were generated to compare the glaucoma detection sensitivity of various parameters. From the ROC curves, we obtained the area under the curve (AUC) of each of the parameters. Statistical analyses were performed using SPSS software version 25.0 (SPSS, Inc., Chicago, IL, USA). $P < 0.05$ indicated statistical significance. In correlation analysis, significant probability values obtained were analyzed for multiple testing using Bonferroni correction ($P < 0.05/3$ indicating statistical significance).

RESULTS

Demographic and Baseline Characteristics of the Study Subjects

This study consecutively enrolled eight healthy individuals and nine patients with POAG. The mean age of healthy and patients with POAG was 63.1 ± 4.0 years (range = 59–71 years) and 65.6 ± 10.2 years (range = 47–83 years), respectively. Mean \pm SD IOPs of the healthy individuals and patients with POAG were 14.0 ± 2.7 mm Hg and 14.3 ± 3.3 mm Hg on an average of 1.6 ± 1.0 IOP-lowering medications, respectively. Baseline characteristics of all participants are shown in Table 1.

Repeatability and Reproducibility of the Measurements of Pulsatile TM Motion

ICCs were assessed to test the agreement of all measurements. The ICCs of IMV, ICDisp, EMV, and ECD for the three consecutive scans in the same eye were 0.965, 0.931, 0.952, and 0.96, respectively, which suggested good repeatability of our measurements. Moreover, the ICCs of IMV, ICDisp, EMV, and ECD, which were analyzed twice on 2 separate sessions over an interval of 2 weeks, were 0.98, 0.972, 0.979, and 0.97, respectively, which also represented a high-level of reproducibility. Because of the high repeatability and reproducibility of the measurements in both our present study and a previous study,¹² we felt that it was satisfactory to use data obtained by one observer (K.G.).

Difference in MV and CDisp Between Healthy Eyes and Eyes with POAG

Figure 2 shows the difference in MV and CDisp between a representative healthy subject and an eye with POAG. Both the maximum velocity and motion amplitude of the TM in the eye with POAG was significantly lower than that in the healthy eye (Supplementary Videos S1 and S2). Box plots showed the measured MV and CDisp for each individual in both groups (Fig. 3). Table 2 summarizes the results for parameters of pulsatile TM motion in the internal and external region of all the recruited eyes in our study. In both regions of the TM, the MV and CDisp in healthy eyes were each significantly higher than those in eyes with POAG (all $P < 0.05$); the mean MV_{mean} and $CDisp_{\text{mean}}$ difference in the result was similar (22.4 ± 5.2 $\mu\text{m/s}$ vs. 13.1 ± 2.6 $\mu\text{m/s}$; $P < 0.001$ for MV_{mean} ; and 0.414 ± 0.25 μm vs. 0.195 ± 0.05 μm ; $P < 0.001$ for $CDisp_{\text{mean}}$). Although the motion signals

TABLE 1. Demographics and Clinical Characteristics

Variable	Healthy Eyes	POAG Eyes	P Value*
Age, y	63.1 ± 4.0	65.6 ± 10.2	0.53
Axial length, mm	23.5 ± 0.9	24.4 ± 1.2	0.025
Anterior chamber depth, mm	3.1 ± 0.3	3.3 ± 0.4	0.06
Cup-to-disc ratio	0.32 ± 0.1	0.82 ± 0.1	<0.01
Mean arterial pressure, mm Hg	98.0 ± 11.4	95.1 ± 17.1	0.69
Heart rate	67.5 ± 11.2	63.9 ± 14.3	0.57
Intraocular pressure, mm Hg	14.0 ± 2.7	14.3 ± 3.3	0.75
Outflow facility, $\mu\text{L}/\text{min}/\text{mm Hg}$	0.42 ± 0.3	0.46 ± 0.4	0.76
Ocular pulse amplitude, mm Hg	3.85 ± 1.4	3.88 ± 1.5	0.96

POAG, primary open-angle glaucoma; SD, standard deviation.

* Unpaired *t*-test.

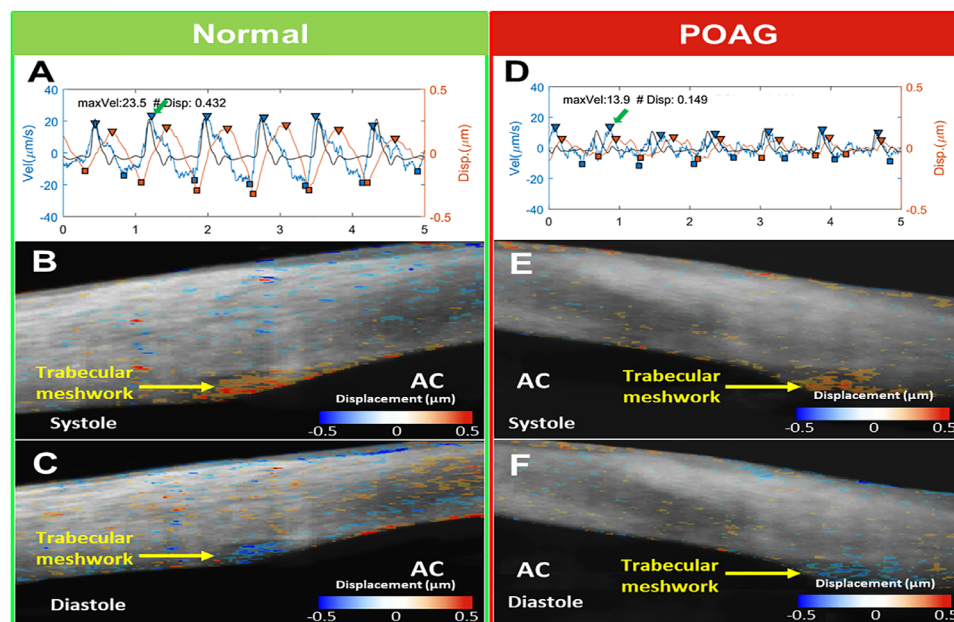


FIGURE 2. Pulsatile trabecular meshwork (TM) movement waveform revealed by phase-sensitive optical coherence tomography (PhS-OCT). Shown are the representative results of pulsatile TM motion in a healthy eye and an eye with POAG. In the healthy eye (A, B, C), instantaneous pulsatile motion of the TM in systole and diastole phases are shown in B and C, respectively. Waveform shown in black lines in A and (D) are the pulsimeter signal. The color heat map illustrates the direction and intensity of the tissue movement. The red color represents the movement anteriorly toward the surface of cornea, whereas the blue color represents the movement posteriorly toward the anterior chamber angle. (E, F) show the instantaneous pulsatile motion in an eye with POAG. (A, D) provide the results of pulsatile TM motion in a healthy eye and an eye with POAG averaged over 5 seconds, respectively. The maximum velocity (green arrow) and motion amplitude (orange line) of the TM in the eye with POAG was significantly lower than that in the healthy eye. POAG, primary open-angle glaucoma; AC, anterior chamber; maxVel, maximum velocity; # Disp, cumulative displacement; Disp, displacement.

of background tissue (i.e. corneoscleral coats) appear to be relatively random, the averaged displacements from both normal and POAG patients were approximately 0.1 μm , markedly smaller than the motion detected at the TM region (Supplementary Fig. S1).

Correlation Analysis Between Pulsatile TM Motion Parameters and Other Ocular Measurements

Pearson's correlation analysis was conducted to determine correlations between pulsatile TM motion parameters and other ocular measurements. Our study found no correlations between pulsatile TM motion parameters and outflow facility. Although MV did not show a good correlation with ocular pulse amplitude, we found a significantly positive correlation between the CDisp and ocular pulse amplitude in all

subjects (Pearson $r = 0.50$; $P = 0.0038$ for ICDisp; Pearson $r = 0.42$; $P = 0.0017$ for ECDisp; Pearson $r = 0.46$; $P = 0.0088$ for CDisp_{mean}; and $P < 0.0167$ indicating statistical significance after Bonferroni correction).

Glaucoma Detection Sensitivity of Various Monitoring Parameters

Figure 4 shows the area under the ROC curves using the values of outflow facility, MV, and CDisp to identify healthy subjects and patients with glaucoma. The ability to discriminate glaucoma from normal parameters was assessed by calculating the AUC; the higher value suggests better discrimination. The diagonal reference line represents a random distribution with an absence of any relationship of clinical value. The outflow facility showed a relatively low

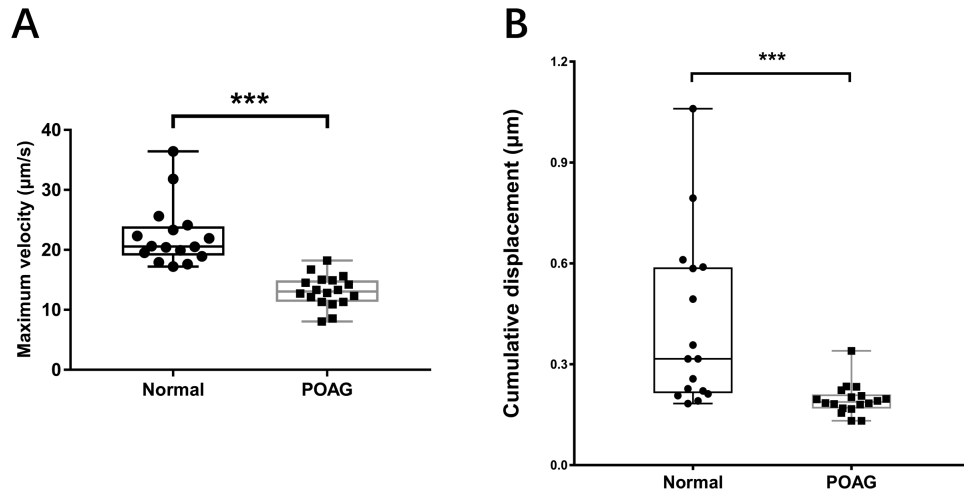


FIGURE 3. Statistical analysis showing measured maximum velocity (A) and cumulative displacement (B) for each individual in the healthy group and POAG group. The mean maximum velocity and cumulative displacement in healthy eyes were significantly higher than those in eyes with POAG. POAG, primary open-angle glaucoma; CDisp, cumulative displacement; MV, maximum velocity. *** $P < 0.001$.

TABLE 2. Comparison of MV and CDisp Between Normal Eyes and Eyes With POAG

Variable	Normal Eyes	POAG Eyes	<i>P</i> Value*
Internal region of the TM			
IMV, $\mu\text{m/s}$	19.4 ± 4.7	10.9 ± 2.3	<0.001
ICDisp, μm	0.33 ± 0.19	0.16 ± 0.05	<0.001
External region of the TM			
EMV, $\mu\text{m/s}$	25.3 ± 5.8	15.3 ± 3.1	<0.001
ECDisp, μm	0.50 ± 0.33	0.23 ± 0.05	<0.001

MV, maximum velocity; CDisp, cumulative displacement; POAG, primary open-angle glaucoma; SD, standard deviation.
*Mann–Whitney *U* test.

discrimination (AUC = 0.521; 95% confidence interval [CI] = 0.321–0.721) as did the IOP (AUC = 0.495; 95% CI = 0.295–0.694). The AUC of the MV (0.990; 95% CI = 0.878–1.000) and CDisp (0.870; 95% CI = 0.710–0.960) showed a significantly better discrimination of glaucoma compared with the outflow facility and the IOP in our study (all $P < 0.05$). In addition, there was no significant difference in the AUC between the outflow facility and the IOP (0.521; 95% CI = 0.321–0.721 vs. 0.495; 95% CI = 0.295–0.694; $P = 0.90$).

DISCUSSION

In this study, we found that eyes with POAG had significantly less pulsatile TM motion compared with healthy eyes using PhS-OCT. Previously, PhS-OCT was used to characterize the parameters of pulse-dependent TM motion and demonstrate its change with accommodation in healthy subjects.¹² The newly observed difference between healthy eyes and eyes with POAG found in this study may be useful in understanding the functional behavior of the AH outflow pathways and in the evaluation and management of glaucoma in clinical practice.

We performed a correlation analysis between parameters of pulsatile TM motion and outflow facility as well as ocular pulse amplitude. CDisp showed good correlation with ocular pulse amplitude whereas MV and CDisp did not correlate with outflow facility, which may be due to

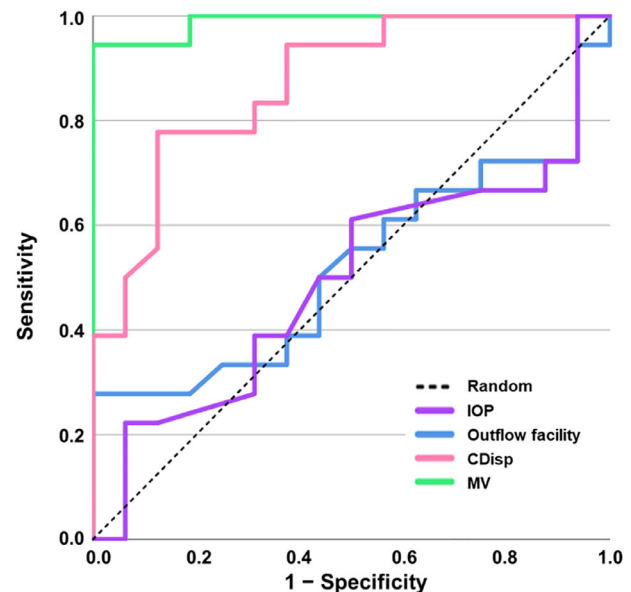


FIGURE 4. Area Under the Receiver Operating Characteristic (AUC) Curves for the Parameters as Shown. The diagonal dotted line displays the random distribution of the null hypothesis associated with a lack of any predictive ability. IOP, indicates intraocular pressure; CDisp, cumulative displacement; MV, maximum velocity.

some limitations of tonography in clinical practice.¹⁷ Significantly improved performance of MV and CDisp AUCs were observed compared with those of either outflow facility or IOP. Tonographic measurement limitations are well known and provide an explanation for the lack of routine use in clinical practice. The difference of glaucoma detection ability that we found suggests PhS-OCT may prove to be a more effective tool than tonography for the evaluation of functional properties of the outflow system.¹⁷

The performance of the AUC for IOP was also less satisfactory than pulsatile parameters in this study, demonstrating its lack of an ability to predict the glaucoma status in contrast to the PhS-OCT measurements. The reason for the

lack of a difference in IOP between the healthy subjects and the patients with POAG may be the use of IOP-lowering medications in glaucoma eyes in our study. In addition, there is ample evidence to suggest that in-office random and infrequent IOP measurements are a poor surrogate for IOP levels throughout the 24 hour period and across multiple visits.^{18–21} Our results are consistent with the evidence that random IOP measurements may not be reflective of the real-time ability of the outflow system to maintain IOP within a narrow range. The pulsatile TM parameters had superior predictive capabilities compared with both outflow facility and the IOP in this study. We recognize that the limited number of subjects in our study permits only a preliminary conclusion, but we feel the findings point to the value of pursuing additional studies.

The ocular pulse results from cardiac cycle induced oscillatory changes in choroidal volume. The pulse waves are transmitted to the entire corneoscleral shell, which must undergo continuous cyclic distention and recoil. However, cyclic motion of the corneoscleral shell was too small for our system to detect. The ocular pulse amplitude reflects the strength of ocular blood flow corresponding to the difference between the minimum and maximum of the pulse wave contour.²² Similarly, the cumulative displacement is the integration of the minimum and maximum of the pulsatile motion corresponding to a cardiac cycle, which consists of both the diastolic and systolic phase. The differences between the analysis associated with velocity and displacement might be the reason CDisp, but not the MV, had a positive correlation with the ocular pulse amplitude. The MV only provided the maximum value of the instantaneous velocity on the velocity waveform.

Previous studies have shown structural differences in the TM between healthy eyes and eyes with POAG using scanning electron microscopy,²³ atomic force microscopy,²⁴ high-frequency ultrasound biomicroscopy,²⁵ and OCT.²⁶ Results of the present clinical research OCT study extend the knowledge to a new parameter; a functional property related to biomechanical changes *in vivo* in the TM of glaucomatous eyes. Pulse-dependent motion of the TM originates from the cardiac pulse through the changes of choroidal vascular volume between systolic and diastolic cardiac pulse waves.²⁷ This pulsatile movement of trabecular meshwork and collector channel in healthy eyes was documented in a recent study using PhS-OCT.¹⁰ Our work is based on the concept of the aqueous pump model with the mechanism described in the latest paper by Lusthaus et al.²⁸ In general, stiffness of the TM depends on the mechanical properties of the sensory arm of the TM cells and their ability to transduce sensory stimuli to alter their own properties as well as their ability to maintain optimal properties of the TM beams and other extracellular matrix components. According to the principles of biomechanics, a stiffer TM would exhibit less tissue deformation than the normal TM.²⁹

The pulsatile movement of the TM due to the pressure difference between the anterior chamber and Schlemm's canal results in pulse-dependent distention and recoil.³⁰ Therefore, an alteration in the composition of the beams, and an accumulation of ECM in the TM interspaces may compromise the pulsatile TM motion in eyes with POAG. Moreover, we speculate that the compromised pulsatile movement of the TM may induce changes in mechanosensing of shear stress or mechanical stretching of the TM,^{31,32} thus establishing a positive feedback loop. Recent study has shown that SC shear stress and TM strain may act as mechanosen-

sory factors for homeostatic regulation of outflow resistance and IOP.³³ This feedback loop may exacerbate malfunction of the TM cells, cause defective modulation of ECM of the TM beams, and also result in excessive accumulation of ECM in the spaces between the beams and in the JCT. Together, these changes may lead to an increase in the resistance to AH outflow and elevation of IOP.^{31,32,34–36}

Depending on differences in outflow facility through the 360 degree circumference of the TM, segmental flow and nonuniform flow patterns were found in both the TM region and distal outflow system.^{7,37} Huang and colleagues demonstrated the segmental pulsatile outflow patterns using aqueous angiography in living nonhuman primates and in living human subjects.^{38,39} Recently, the TM-targeted microinvasive glaucoma surgery (MIGS) and new IOP-lowering drugs have received increasing attention from researchers. For instance, a trabecular micro-bypass system was implanted through the TM into Schlemm's canal, resulting in improvement of AH outflow and a reduction of IOP.⁴⁰ MIGS implants were shown to be safer and had a smaller surgical incision compared with conventional glaucoma surgeries in several recent studies.^{41,42} Ideally, the PhS-OCT technique could examine 360 degrees of the limbal circumference preoperatively to determine desirable regions for MIGS usage. Distal outflow is more likely to be intact in regions exhibiting normal pulsatile motion, which may provide better outcomes.⁴³ On the other hand, it might be better to treat an area without good pulsatile movement, thus sparing the area with more normal function. The optimal strategy for this awaits further study. Theoretically, with PhS-OCT, we could accurately select the TM region based on an optimized strategy, thus offering the potential for customizing TM-based glaucoma surgeries.

Moreover, Rho-associated protein kinase (ROCK) inhibitors were developed as a novel class of medications to lower IOP in patients with glaucoma, and were approved for the treatment of glaucoma in the United States in 2017. These ROCK inhibitors act to significantly increase outflow facility or decrease outflow resistance (i.e. decreasing the density of actin stress fibers, modifying the cytoskeleton of the TM cells to be less stiff, and relaxing smooth muscle cells in the TM region).^{44–47} Although IOP is an indirectly derived surrogate for the behavior of the outflow system, it does not provide a definitive functional assessment. Therefore, real-time TM-targeted parameters other than IOP are needed to evaluate the changes in the TM behavior following the use of novel IOP-lowering medications and MIGS. PhS-OCT, through its ability to detect dynamic TM motion represents such a parameter. Our future studies will focus on evaluation of the pulsatile motion over the entire circumferential TM tissue and changes in TM pulsatile movement in patients with glaucoma as a result of instillation of TM-targeted glaucoma medications and MIGS.

Limitations

There are several limitations in this study. (1) Our present study investigated the difference in pulsatile TM motion between healthy eyes and eyes with POAG. Whether there are changes in the pulsatile movement of the TM in patients with glaucoma and in different stages of POAG will require further cross-sectional and longitudinal studies. (2) Another potential limitation of our study was that the patients with glaucoma were all under treatment with pressure-lowering medications. The medications may affect not only pressures

and facility but also the biomechanics related to TM motion. Despite the presence of medication-lowering agents and lower pressures, PhS-OCT was effective in identifying patients with glaucoma. The study suggests that neither lower IOP nor the presence of medications restores abnormal biomechanical properties identified by our studies of TM motion. An additional limitation of this initial feasibility study is that we only examined the temporal quadrant. The results of this study appear sufficiently promising that we are planning a future study to determine variability of motion around the entire circumference of the limbus. Last, repeatability in this study was assessed using a single operator; future studies will also be needed to assess inter-user repeatability.

CONCLUSIONS

In this study, pulsatile TM motion in healthy eyes was found to be significantly greater than in glaucoma eyes using PhS-OCT. The reduced motion may be due to the altered tissue stiffness or other biomaterial properties of the TM in eyes with POAG. Imaging the pulsatile TM motion may provide new insights into glaucoma pathophysiology and may also be useful in the clinical management of glaucoma.

Acknowledgments

The authors thank the coordination assistance of Francy Moses for this study.

Meeting presentation: Presented in part at the Association for Research in Vision and Ophthalmology Annual Meeting, Vancouver, BC, Canada, April 28 to May 2, 2019.

Supported by the Washington Research Foundation (Wang), Carl Zeiss Meditec Inc. (Wang), Latham grant (Joanne C. Wen), the Fundamental Research Funds of the State Key Laboratory of Ophthalmology (30306020240020315), the Medical Scientific Research Foundation of Guangdong Province (A2020075), and an unrestricted departmental grant from Research to Prevent Blindness.

Role of the Funder/Sponsor: The funder had no role in the design and conduct of the study, collection, management, analysis, and interpretation of the data, preparation, review, or approval of the manuscript, and decision to submit the manuscript for publication.

Disclosure: **K. Gao**, None; **S. Song**, None; **M.A. Johnstone**, None; **Q. Zhang**, None; **J. Xu**, None; **X. Zhang**, None; **R.K. Wang**, Oregon Health and Science University and the University of Washington (N), Carl Zeiss Meditec Inc. (F), Moptim Inc. (F), Colgate Palmolive Company (F), and Facebook Technologies LLC (F), Carl Zeiss Meditec (C), Johnson & Johnson Vision Care (C), and Insight Photonic Solutions (C). **J.C. Wen**, None

References

- Quigley HA, Broman AT. The number of people with glaucoma worldwide in 2010 and 2020. *Br J Ophthalmol*. 2006;90:262–267.
- Tham YC, Li X, Wong TY, Quigley HA, Aung T, Cheng CY. Global prevalence of glaucoma and projections of glaucoma burden through 2040: a systematic review and meta-analysis. *Ophthalmology*. 2014;121:2081–2090.
- Gordon MO, Beiser JA, Brandt JD, et al. The Ocular Hypertension Treatment Study: baseline factors that predict the onset of primary open-angle glaucoma. *Arch Ophthalmol*. 2002;120:714–720.
- Bahrami H. Causal inference in primary open angle glaucoma: specific discussion on intraocular pressure. *Ophthalmic Epidemiol*. 2006;13:283–289.
- Dastiridou AI, Tsironi EE, Tsilimbaris MK, et al. Ocular rigidity, outflow facility, ocular pulse amplitude, and pulsatile ocular blood flow in open-angle glaucoma: a manometric study. *Invest Ophthalmol Vis Sci*. 2013;54:4571–4577.
- Tamm ER, Fuchshofer R. What increases outflow resistance in primary open-angle glaucoma? *Surv Ophthalmol*. 2007;52(suppl 2):S101–S104.
- Stamer WD, Acott TS. Current understanding of conventional outflow dysfunction in glaucoma. *Curr Opin Ophthalmol*. 2012;23:135–143.
- Keller KE, Aga M, Bradley JM, Kelley MJ, Acott TS. Extracellular matrix turnover and outflow resistance. *Exp Eye Res*. 2009;88:676–682.
- Stamer WD, Clark AF. The many faces of the trabecular meshwork cell. *Exp Eye Res*. 2017;158:112–123.
- Xin C, Johnstone M, Wang N, Wang RK. OCT study of mechanical properties associated with trabecular meshwork and collector channel motion in human eyes. *PLoS One*. 2016;11:e0162048.
- Carreon T, van der Merwe E, Fellman RL, Johnstone M, Bhattacharya SK. Aqueous outflow - a continuum from trabecular meshwork to episcleral veins. *Prog Retin Eye Res*. 2017;57:108–133.
- Xin C, Song S, Johnstone M, Wang N, Wang RK. Quantification of pulse-dependent trabecular meshwork motion in normal humans using phase-sensitive OCT. *Invest Ophthalmol Vis Sci*. 2018;59:3675–3681.
- Shin JW, Sung KR, Park SW. Patterns of progressive ganglion cell-inner plexiform layer thinning in glaucoma detected by OCT. *Ophthalmology*. 2018;125:1515–1525.
- Wang RK, Kirkpatrick S, Hinds M. Phase-sensitive optical coherence elastography for mapping tissue microstrains in real time. *Applied Physics Letters*. 2007;90:164105.
- An L, Chao J, Johnstone M, Wang RK. Noninvasive imaging of pulsatile movements of the optic nerve head in normal human subjects using phase-sensitive spectral domain optical coherence tomography. *Opt Lett*. 2013;38:1512–1514.
- An L, Wang RK. In vivo volumetric imaging of vascular perfusion within human retina and choroids with optical micro-angiography. *Opt Express*. 2008;16:11438–11452.
- Johnstone MA. Aqueous humor outflow system Overview. In: Stamper RL, Lieberman MF, Drake MV, eds. *Becker-Schaffer's Diagnosis and Therapy of the Glaucomas*. New York, NY: Elsevier Health Sciences; 2009:39–41.
- Barkana Y, Anis S, Liebmann J, Tello C, Ritch R. Clinical utility of intraocular pressure monitoring outside of normal office hours in patients with glaucoma. *Arch Ophthalmol*. 2006;124:793–797.
- Fogagnolo P, Orzalesi N, Ferreras A, Rossetti L. The circadian curve of intraocular pressure: can we estimate its characteristics during office hours? *Invest Ophthalmol Vis Sci*. 2009;50:2209–2215.
- Jiang X, Torres M, Varma R, Los Angeles Latino Eye Study Group. Variation in intraocular pressure and the risk of developing open-angle glaucoma: the Los Angeles Latino Eye Study. *Am J Ophthalmol*. 2018;188:51–59.
- Sultan MB, Mansberger SL, Lee PP. Understanding the importance of IOP variables in glaucoma: a systematic review. *Surv Ophthalmol*. 2009;54:643–662.
- Kaufmann C, Bachmann LM, Robert YC, Thiel MA. Ocular pulse amplitude in healthy subjects as measured by dynamic

- contour tonometry. *Arch Ophthalmol*. 2006;124:1104–1108.
23. Sihota R, Goyal A, Kaur J, Gupta V, Nag TC. Scanning electron microscopy of the trabecular meshwork: understanding the pathogenesis of primary angle closure glaucoma. *Indian J Ophthalmol*. 2012;60:183–188.
 24. Last JA, Pan T, Ding Y, et al. Elastic modulus determination of normal and glaucomatous human trabecular meshwork. *Invest Ophthalmol Vis Sci*. 2011;52:2147–2152.
 25. Yan X, Li M, Chen Z, Zhu Y, Song Y, Zhang H. Schlemm's canal and trabecular meshwork in eyes with primary open angle glaucoma: a comparative study using high-frequency ultrasound biomicroscopy. *PLoS One*. 2016;11:e0145824.
 26. Wang K, Johnstone MA, Xin C, et al. Estimating human trabecular meshwork stiffness by numerical modeling and advanced OCT imaging. *Invest Ophthalmol Vis Sci*. 2017;58:4809–4817.
 27. Johnstone M, Martin E, Jamil A. Pulsatile flow into the aqueous veins: manifestations in normal and glaucomatous eyes. *Exp Eye Res*. 2011;92:318–327.
 28. Lusthaus JA, Khatib TZ, Meyer PAR, McCluskey P, Martin KR. Aqueous outflow imaging techniques and what they tell us about intraocular pressure regulation [published online ahead of print August 21, 2020]. *Eye (Lond)*, <https://doi.org/10.1038/s41433-020-01136-y>.
 29. Wang K, Read AT, Sulchek T, Ethier CR. Trabecular meshwork stiffness in glaucoma. *Exp Eye Res*. 2017;158:3–12.
 30. Johnstone MA. Intraocular pressure regulation: findings of pulse-dependent trabecular meshwork motion lead to unifying concepts of intraocular pressure homeostasis. *J Ocul Pharmacol Ther*. 2014;30:88–93.
 31. Tumminia SJ, Mitton KP, Arora J, Zelenka P, Epstein DL, Russell P. Mechanical stretch alters the actin cytoskeletal network and signal transduction in human trabecular meshwork cells. *Invest Ophthalmol Vis Sci*. 1998;39:1361–1371.
 32. Vittal V, Rose A, Gregory KE, Kelley MJ, Acott TS. Changes in gene expression by trabecular meshwork cells in response to mechanical stretching. *Invest Ophthalmol Vis Sci*. 2005;46:2857–2868.
 33. Sherwood JM, Stamer WD, Overby DR. A model of the oscillatory mechanical forces in the conventional outflow pathway. *J R Soc Interface*. 2019;16:20180652.
 34. Luna C, Li G, Qiu J, Challa P, Epstein DL, Gonzalez P. Extracellular release of ATP mediated by cyclic mechanical stress leads to mobilization of AA in trabecular meshwork cells. *Invest Ophthalmol Vis Sci*. 2009;50:5805–5810.
 35. Junglas B, Kuespert S, Seleem AA, et al. Connective tissue growth factor causes glaucoma by modifying the actin cytoskeleton of the trabecular meshwork. *Am J Pathol*. 2012;180:2386–2403.
 36. Vranka JA, Acott TS. Pressure-induced expression changes in segmental flow regions of the human trabecular meshwork. *Exp Eye Res*. 2017;158:67–72.
 37. Chang JY, Folz SJ, Laryea SN, Overby DR. Multi-scale analysis of segmental outflow patterns in human trabecular meshwork with changing intraocular pressure. *J Ocul Pharmacol Ther*. 2014;30:213–223.
 38. Huang AS, Li M, Yang D, Wang H, Wang N, Weinreb RN. Aqueous angiography in living nonhuman primates shows segmental, pulsatile, and dynamic angiographic aqueous humor outflow. *Ophthalmology*. 2017;124:793–803.
 39. Huang AS, Camp A, Xu BY, Penteado RC, Weinreb RN. Aqueous angiography: aqueous humor outflow imaging in live human subjects. *Ophthalmology*. 2017;124:1249–1251.
 40. Huang AS, Penteado RC, Papoyan V, Voskanyan L, Weinreb RN. Aqueous angiographic outflow improvement after trabecular microbypass in glaucoma patients. *Ophthalmology Glaucoma*. 2019;2:11–21.
 41. Samuelson TW, Chang DF, Marquis R, et al. A Schlemm canal microstent for intraocular pressure reduction in primary open-angle glaucoma and cataract: the HORIZON study. *Ophthalmology*. 2019;126:29–37.
 42. Samuelson TW, Sarkisian SR, Lubeck DM, et al. Prospective, randomized, controlled pivotal trial of iStent inject trabecular micro-bypass in primary open-angle glaucoma and cataract: two-year results. *Ophthalmology*. 2019;126(6):811–821.
 43. Teng CC, Paton RT, Katzin HM. Primary degeneration in the vicinity of the chamber angle; as an etiologic factor in wide-angle glaucoma. *Am J Ophthalmol*. 1955;40:619–631.
 44. Tanna AP, Johnson M. Rho kinase inhibitors as a novel treatment for glaucoma and ocular hypertension. *Ophthalmology*. 2018;125:1741–1756.
 45. Thieme H, Nuskovski M, Nass JU, Pleyer U, Strauss O, Wiederholt M. Mediation of calcium-independent contraction in trabecular meshwork through protein kinase C and rho-A. *Invest Ophthalmol Vis Sci*. 2000;41:4240–4246.
 46. Honjo M, Tanihara H, Inatani M, et al. Effects of rho-associated protein kinase inhibitor Y-27632 on intraocular pressure and outflow facility. *Invest Ophthalmol Vis Sci*. 2001;42:137–144.
 47. Ren R, Li G, Le TD, Kocczynski C, Stamer WD, Gong H. Netarsudil increases outflow facility in human eyes through multiple mechanisms. *Invest Ophthalmol Vis Sci*. 2016;57:6197–6209.

SUPPLEMENTARY MATERIAL

SUPPLEMENTARY VIDEOS S1 AND S2. The supplementary videos show dynamic tissue displacements experienced by the TM relative to motion of the surrounding tissue over a period of 3 seconds. The TM clearly experiences pulsatile motion identical to the heart-beat frequency. The patient with POAG shows a lower magnitude of motion compared to the healthy subject.